Received: 15 March 2017 | Revised: 17 August 2017 | Accepted: 2 January 2018

DOI: 10.1002/we.2170

RESEARCH ARTICLE

WILEY

Intermediate layer as measure against rolling bearing creep

T. Schiemann[1] | **S. Pörsch**[2] | **E. Leidich**[1] | **B. Sauer**[2]

[1]Technische Universität Chemnitz, Reichenhainer Str. 70, 09126 Chemnitz, Germany

[2]Technische Universität Kaiserslautern, Gottlieb-Daimler-Straße 42, 67663 Kaiserslautern, Germany

Correspondence
T. Schiemann, Technische Universität Chemnitz, Reichenhainer Str. 70, 09126 Chemnitz, Germany.
Email: tom.schiemann@mb.tu-chemnitz.de

Funding information
AiF [German Federation of Industrial Research Associations]

Abstract

Rolling bearings are a part of every wind-turbine transmission. In terms of bearing design, the bearing rings are of particular interest. The current trend for increasing power and dynamic stress, together with the associated increases in specific loads, have brought creep—an irreversible relative motion between bearing rings and shafts or housings—to the forefront. Creep leads to wear and can cause shaft displacements with serious consequences for the meshing of teeth in gearboxes, for example. In fact, many insurance companies cite the creep of bearing rings as one of the main causes of wind-turbine gearbox failures.

This article presents a complex kinematic 3D FE multi-body simulation of a rolling bearing. This simulation makes a detailed analysis of the relative motion or creep of bearing rings possible for the first time.

It also presents options, based on materials technology and design, for reducing or eliminating creep in existing systems or at the product-development phase. The 2 key solutions, both based on an additional layer between bearing and housing, that show best results are presented within this article. This gives the user specific information for optimizing the bearing structure with respect to the choice of bearing and bearing ring design to ensure that future damage is prevented.

KEYWORDS

bearing creep, fretting corrosion, intermediate layer, measure against rolling bearing creep, rolling bearing

1 | INTRODUCTION AND PROBLEM DEFINITION

The lifespan of many drive units is determined, among other things, by the lifespan of the rolling bearings installed. In order to achieve a high reliability for the entire system, it is necessary to harmonize all components and action pairs that lie in the flux of force. In terms of rolling bearings, this puts the focus on the rolling bearing seats, which are directly and indirectly exposed to radial, bending, and torsional loads.

As a consequence of the constantly increasing specific loads acting on the rolling bearing, there is an increasing range of damage scenarios that can be attributed to significant relative motion associated with ring creep.[1-3] The consequent slipping motion leads to fretting and/or massive wear.[4] Often, bearing failures due to bearing creep are mentioned in the context of wind turbines,[5] gearbox bearings as well as main rotor shaft bearings. More and more designers of automotive gearboxes, electric motors, and auxiliary units in aviation industry have to struggle with creep induced bearing failures.

Ring creep is a caterpillar-like walking motion of the bearing ring that, in contrast to tangential slippage in shaft-hub interference fits, occurs even without the nominal transfer of torque. Figure 1 illustrates the creeping process in detail. The figure shows the outer ring of a bearing, the rolling elements, and the housing and is divided into 2 parts, showing a stationary bearing (top) and a moving bearing (bottom). It is clear that even a purely normal load (with the bearing at rest) causes a major deformation of the bearing ring as shown (top). The bearing is radially compressed in the areas under load, and outside these areas it is both radially and tangentially stretched. Accordingly, volume is displaced from the loaded zone into the regions between the rolling elements. Consequently, the bearing ring elongates and bulges out, causing a partial reduction in the joint pressure. Furthermore, there are strong shear stresses in this area of the bearing seat. If the bearing then starts to rotate (bottom), there is a directional compression of the bearing ring in the direction of rotation. Localized slippage then occurs if the critical value of shear stress for creep is exceeded in this region of the bearing seat. On further rotation of the bearing, this results in a continuous displacement (creeping motion) between the

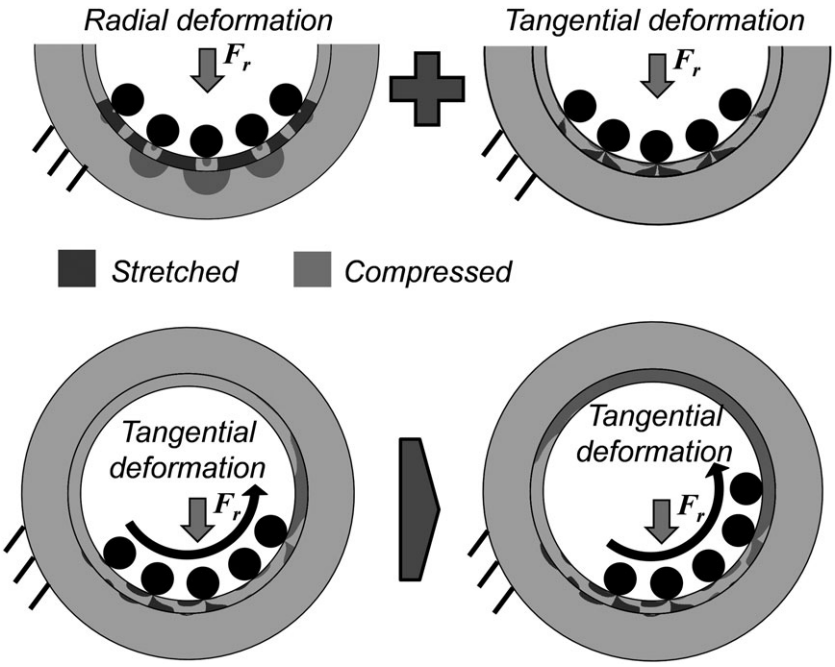

FIGURE 1 Creeping motion as a result of bearing-ring deformation[3]

bearing ring and the surrounding geometry. This ring creep phenomenon needs to be distinguished from the creep phenomenon that takes place in planetary gear wheels that is a result of the ovalization of the planetary gear wheel.[6]

Research project[1] of the Forschungsvereinigung Antriebstechnik e.V. (FVA) revealed the creep of outer rings under point loads due to a complex interaction between the prevailing boundary conditions to be particularly critical. Furthermore, Leidich et al[1] investigated significant influencing variables for radial bearings. Figure 2 summarizes the relevant variables and assesses them qualitatively in terms of their influence on the tendency of a bearing to creep.

Based on these findings, Leidich et al[2] investigated various bearing types with regard to their tendency to creep. It was found that tapered roller bearings and angular-contact ball bearings are the designs that have the highest creep threshold. Cylindrical roller bearings and spherical roller bearings have comparatively lower creep thresholds and are therefore more susceptible to creep. The most creep-susceptible bearing type is the deep groove ball bearing.

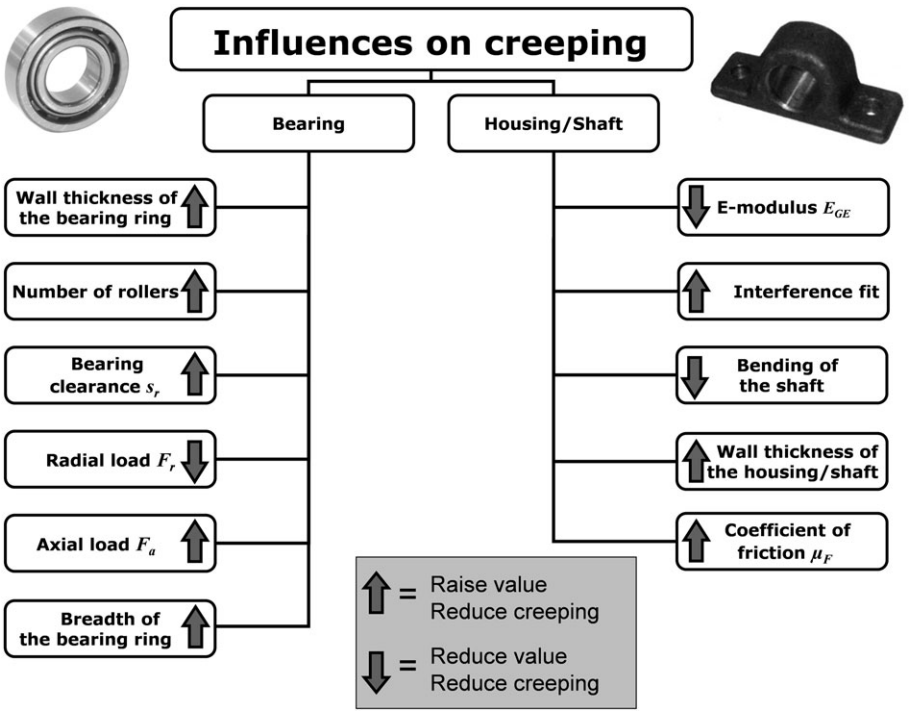

FIGURE 2 Overview and assessment of design-based measures against creep[2]

These comprehensive research projects have provided a foundation for eliminating rolling bearing creep in the early design phase by simple means (design measures). The tendency of a bearing to creep can be significantly reduced by considering these influencing variables. However, due to high specific bearing loads or other constraints, there are cases where these measures are either insufficient or unable to be implemented. In such cases, the designer needs to have access to secondary measures that guarantee that bearing ring creep can be reliably ruled out in a specific application.

2 | MEASURES AGAINST ROLLING BEARING CREEP

Based on the knowledge generated within the previous projects, several tribological and design measures against rolling bearing creep were developed. The first measures aim at an increasing friction coefficient μ_F in the joint to increase the friction force and thus counteract the bearing creep. Therefore, a laser structuring of the outer ring of the bearing and different housing materials were investigated. As a first version of the intermediate layers, elastic layers for instance, a glass fiber-reinforced plastic (GRP) on the outer ring was tested. The elastic layer absorbs the ring deformation which results in a reduction of bearing creep. Another intermediate layer is a steel ring which will be described in the following section. As a positive connection measures, cylindrical pins, which are inserted in grooves in the outer ring, were tested. Specifically engineered retaining rings were developed to prevent rolling bearings from rolling bearing creep. Figure 3 gives an overview of the previously described measures.

These measures were all investigated with complex 3D FEM analysis as well as experimental tests for a constant verification. Within this article only the investigation for intermediate layers will be given. The results of the analysis of all measures are provided in Sauer et al.[7]

The following sections contain the description of the 3D FEM analysis methods and the experimental investigation.

3 | FINITE ELEMENT ANALYSIS

The comprehensive investigation of the measures presented herein required the creation of extensive FE models. These highly complex, computationally demanding 3D kinematic models to recreate real creep phenomena were constructed using the simulation methodology presented in Maiwald.[8] For these FE analyses, version 6.12-1 of the ABAQUS software (implicit solver) was used. Access to the Chemnitz High-Performance Linux Cluster ("CHiC") provides the requisite technical background to be able to calculate even tasks defined by the wind-energy industry with this simulation methodology.

These conditions made it possible to investigate several measures, only excerpts of which are presented here, and to look into their effects on creep behavior. The focus of these investigations was on deep groove ball bearings of types 6205 and 6216 and on cylindrical roller bearings of types NU205 and NU216 (see Figure 4). A cylindrical housing was primarily used for the simulative and also for the experimental studies. All simulations were carried out on outer rings under point loads.

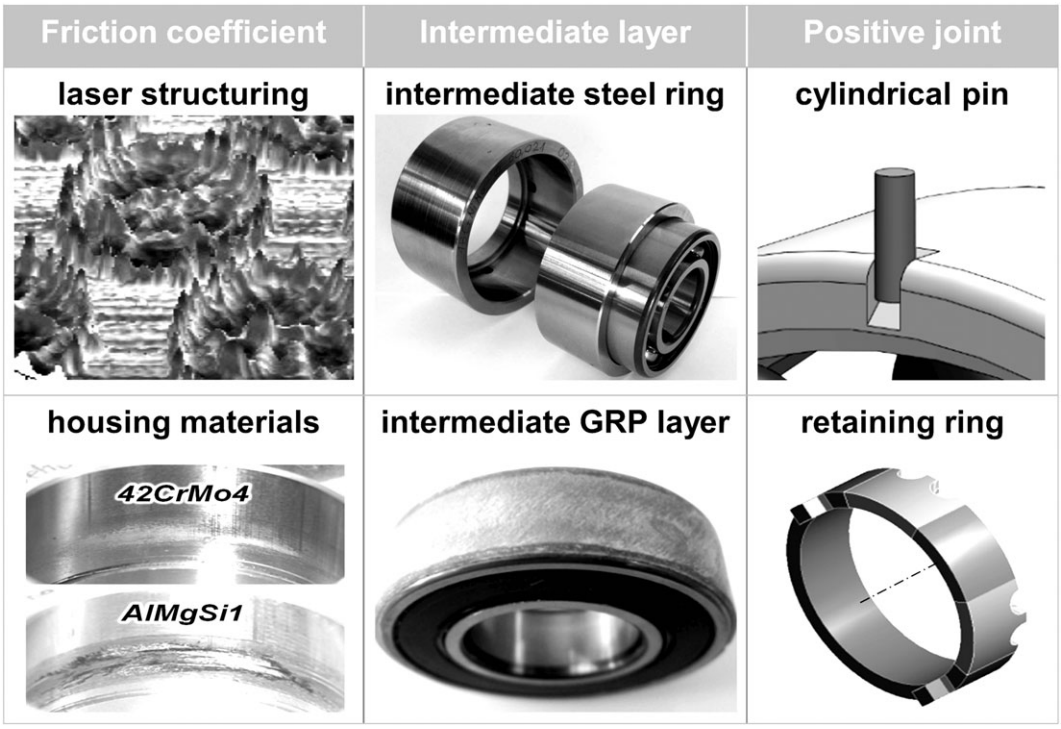

FIGURE 3 Overview of measures against rolling bearing creep

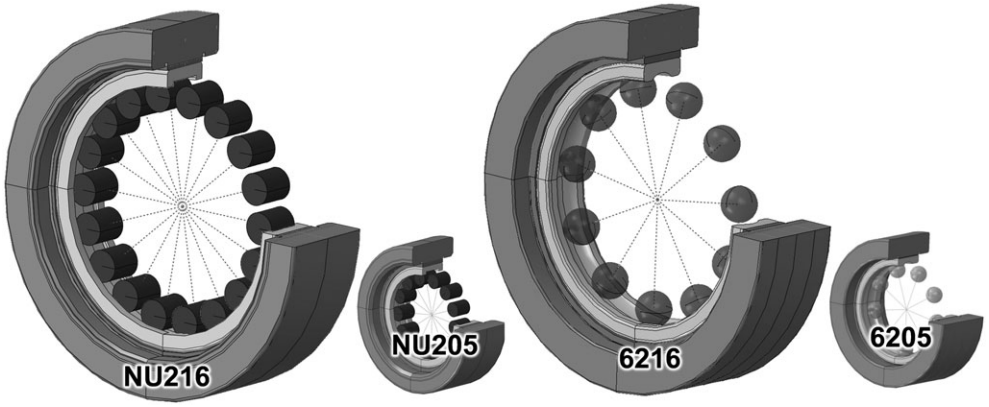

FIGURE 4 Cutaway diagrams of simulated bearing versions

3.1 | Model setup

Figure 5 shows the model setup using a 3D cutaway model of deep groove ball bearing of type 6205 and the simplifications made with respect to the rolling element cage. It is clear that some simplifications (with negligible impact on the precision regarding creep behavior) were undertaken in the calculation models. Thus, only the respective bearing ring, intermediate ring, or intermediate layer with housing and rolling elements were simulated. The housing, intermediate ring, or intermediate layer and bearing ring are defined as independent elastic bodies with the material properties in Table 1. This bodies are simulated using approximately 270 000 linear hexahedral elements (C3D8R) and 30 000 linear wedge elements (C3D6). The rolling elements were modeled as rigid bodies. After arranging the individual components in the overall model, the respective reference points of all the rolling elements were coupled with a central reference point (center point) using sliders (*connector type "translator"*) (Figure 5 right). Thus, each rolling element has only 1 remaining degree of freedom in the radial direction. This degree of freedom is then eliminated in the form of force constraints or rolling element loads, which can be calculated according to DIN ISO 281.[9] By rotating the center point, the rolling elements move in the circumferential direction and glide frictionless over the contact surface of the outer ring. A detailed explanation of the model setup and functioning can be found in Leidich et al,[2] Maiwald,[8] and Leidich and Maiwald.[10] This simulation methodology allows several revolutions of a rolling bearing to be represented using the FEM. In addition to a precise evaluation of the processes in the contact joint, this also allows an extensive variation of parameters.

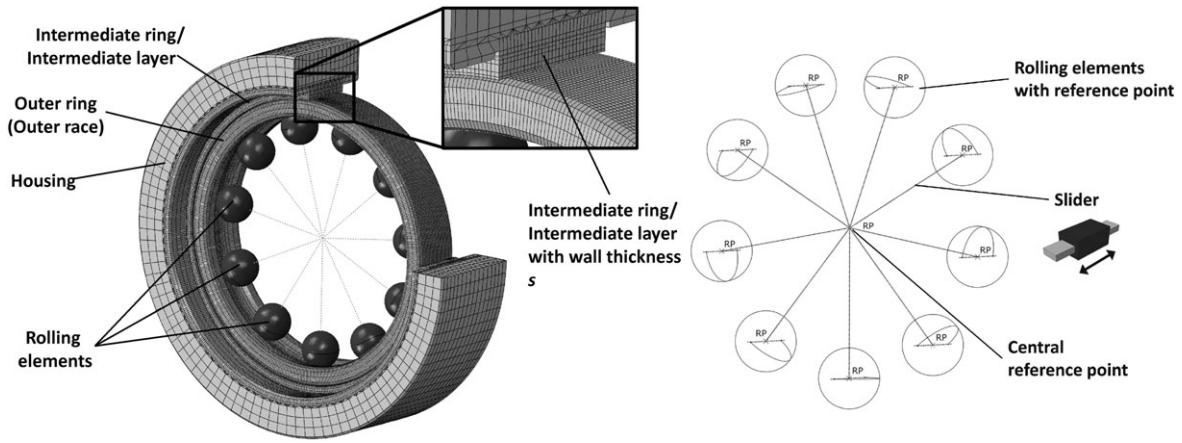

FIGURE 5 FE cutaway model of a deep-groove ball bearing with intermediate ring (left); connector type: "Translator" between the central reference node (center point) and the rolling elements (rigid bodies) (right)

TABLE 1 Material properties of the bearing ring, housing, and plastic coating

Material	Young's Modulus, N/mm^2 E_{GE}; E_{FDD}	Poisson's Ratio ν, –
42CrMo4 / 100Cr6 (intermediate ring / bearing ring)	210 000	0.3
GJS 600 (housing)	170 000	0.28
Plastic (intermediate layer)	5000	0.35

3.2 | Anisotropic material behavior

Two versions of the elastic intermediate layer inserted in the bearing seat were investigated. This was applied to the bearing as a thermoplastic with isotropic material behavior (polyethylene-vinyl acetate copolymer—PEVAC) and also as a GRP layer with anisotropic material behavior. In the case of the GRP layer, the material is orthotropic, exhibiting a special form of anisotropy. The "engineering constants" (Abaqus) material model was used to depict this material behavior. For this model, every point in the elastic layer must be assigned a local coordinate system (see Figure 6). Using this coordinate system, the material properties in Table 2 are then plotted in the respective direction.

3.3 | Verification

The numerical simulations were accompanied by experiments at the Institute of Machine Elements, Gears and Transmissions at the University of Kaiserslautern in order to provide a verification of the simulation.[7] The creep force, F_C, the creep torque, T_C, and the creep threshold, $p_{r,lim}$ ($F_{r,lim}$) were chosen as suitable variables for comparing experiment and simulation. T_C describes the torque acting along the circumference that arises from the prevention of the tangential relative motion between the housing and the bearing ring (see Figure 7). Thus, T_C represents the torque that cannot be absorbed by the housing due to the prevailing frictional fit. The creep threshold is defined as the radial load of the bearing at which the bearing starts to creep.

The bearing seat fit is stated as the related clearance, ξ^*, which is calculated from the (nominal) joint diameter, d_F, and the difference Δd between the outer ring diameter d_{OR}, and the Housing diameter d_H.

$$\xi^* = \frac{d}{d_F} = \frac{d_{OR} - d_H}{d_F}$$

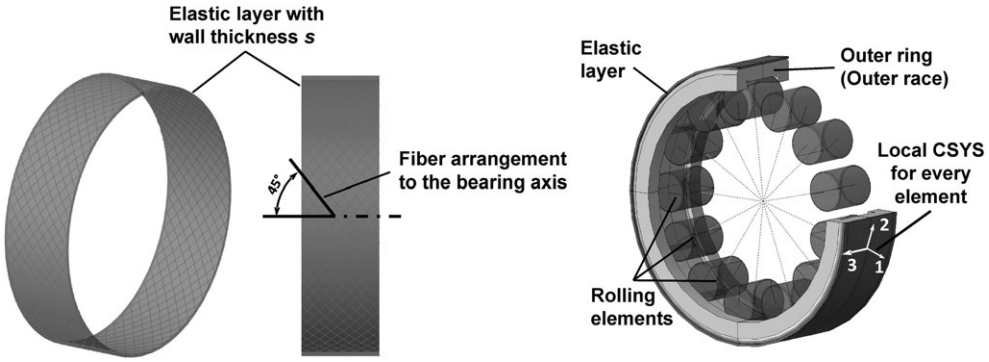

FIGURE 6 Fiber orientation in the elastic layer (left); local coordinate systems in the elastic layer (right)

TABLE 2 Material properties of the layer with orthotropic material behavior with regard to the coordinate system presented in Figure 7

Material	$E_1 = E_2$, GPa	E_3, GPa	$G_{12} = G_{23} = G_{13}$, GPa	ν_{12}, –	$\nu_{23} = \nu_{13}$, –
GRP	22.72	6.86	2.55	0.0805	0.265

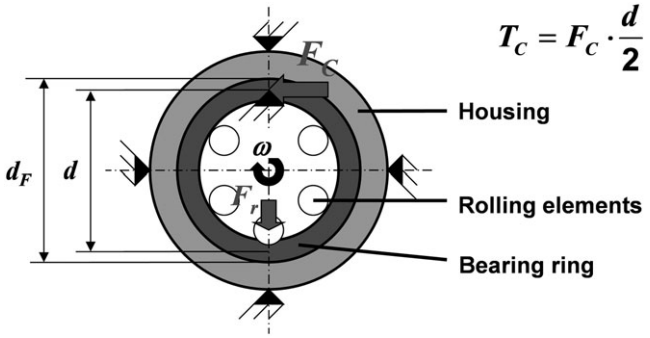

FIGURE 7 Definition of the creep force F_C, the creep torque T_C, and the radial load F_r[8]

The radial load is also stated as a related variable and is calculated from the radial load F_r and the projected bearing seat area A_{proj}.

$$p_r = \frac{F_r}{A_{proj}}$$

4 | EXPERIMENTAL INVESTIGATION

For the verification of the numerical simulation, different test benches were used in order to investigate rolling bearing creep of the bearing outer ring under point load. Important verification variables are the bearing ring creep threshold as well as the creep torque. Thus, the test benches were customized to enable the detection of both. Deep groove ball bearings 6205 and cylindrical roller bearings NU205 were investigated with the "Vario-Shaft" test bench which is shown in Figure 8.

The test-bearing (1) is located in the test-housing (2) which is placed within the radial load unit (3), where the load is applied through a disc spring pack (4) and measured by a load cell (5). It is also possible to mount a hydraulic actuator to apply the radial load which enables a dynamic load. In this configuration of the test bench, the housing is fixed, and the bearing is driven by the test-shaft (6) which is connected to the drive shaft (7). The drive shaft is supported by the bearing (8) and (9).

A second test bench which is usually used to investigate the frictional moment of rolling bearings is used for investigating larger deep groove ball bearings 6216. Figure 9 shows the "Frictional torque test bench."

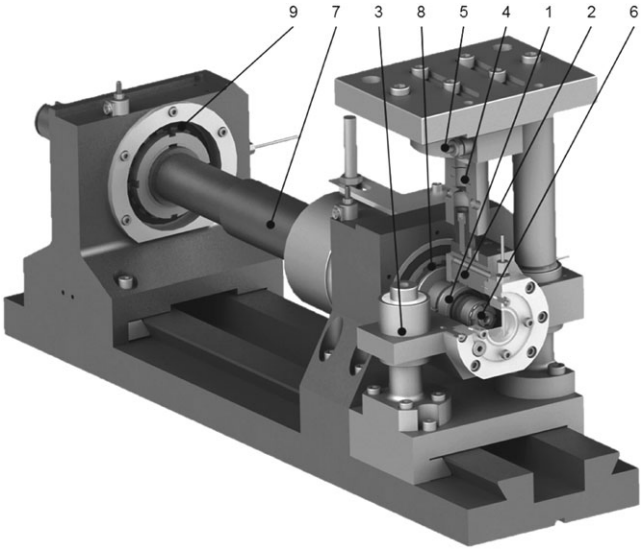

FIGURE 8 "Vario-shaft" test bench

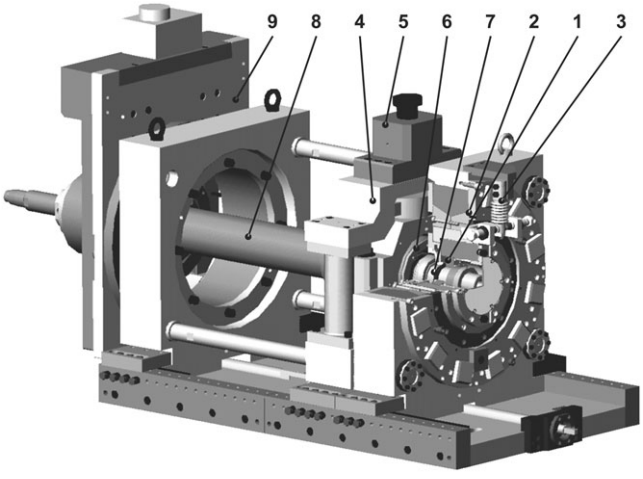

FIGURE 9 Frictional torque test bench

The test bearing (1) is located within the hydrostatic bearing (2). A bending beam (3) is used to hold the hydrostatic bearing in place and to measure the frictional torque of the test bearing. The radial load is applied onto the shaft by the load unit (4). A disc spring pack (5) initiates the radial load through a load cell and a second bearing (6) to the shaft (7). The shaft is connected to the drive shaft (8) which is driven by a belt drive that is placed behind the second support unit (9).

To detect the bearing creep, a transducer is installed on the outer ring of the test bearing, see Figure 10. An inductive sensor (switching distance 2 mm, switching frequency 1.5 kHz) is placed in front of the transducer that delivers a constant voltage signal that drops when a metallic object is within the switching distance of the sensor. Thus, it is possible to count the number of the teeth of the transducer that passes the sensor and to count back to the speed of the bearing outer ring. Thereby, not only the bearing creep threshold can be detected by slowly applying the radial load, but also the bearing creep speed and the outer ring revolutions can be detected. This procedure can be used with both test benches.

For detecting the bearing creep torque, 2 different methods were carried out and customized to the test bench used. For the "Vario-shaft" test bench, a rotatable mounted lever is used, which with 1 end is fixed to the bearing outer ring and the other end is pressing a load cell (nominal force: 500 N, linearity deviation: <0.2%). Thus, it is possible to measure the force that is required to prevent the bearing from creeping, the creep force. Knowing the radial position of the lever allows the calculation of the creep torque.

Using the frictional torque test bench, a torque meter is used and connected to the bearing outer ring by a special flange. This torque meter (nominal torque: 100 Nm, linearity deviation: 0.1%) directly delivers the torque that is necessary to prevent the bearing from creeping (creep torque). All signals were filtered with a low-pass filter with a frequency of 10 Hz.

Table 3 gives an overview of the geometrical and load-related parameters of the bearings that were investigated during the research.

As mentioned before the related clearance, ξ^*, and the related load, p_r, are the most relevant parameters describing the bearing with regard to its tendency to creep. Therefore, the diameters of the housings and the bearings were measured. The influence of the fit clearance was investigated in Leidich et al.[2] In regard to the measures, clearance fits with a high tendency to creep were used to ensure bearing creep. The influence of the radial force was also investigated in Leidich et al[1] and was set to a creep-critical area for this project, see Table 4. The tests were conducted with a constant shaft speed of 3000 rpm as the shaft speed has no influence of the bearings tendency to creep.[2] During the tests, the bearings were lubricated with an oil bath consisting of a non-additive mineral oil of class ISO VG 100. After approximately 80 000 revolutions, the operating temperature of 50°C–60°C, as equilibrium between frictional heat and convection cooling, was reached. To evaluate the measures, the average roughness value Ra and peak-to-valley-height Rz of the bearings and housings were measured before and after the tests. Measured were the bearings seating surfaces of the housing and bearing in axial direction. The procedure was performed by DIN EN ISO 4287.

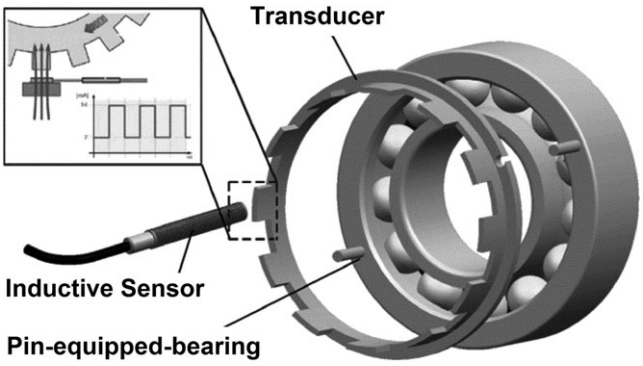

FIGURE 10 Measuring principle for detection of bearing creep

TABLE 3 Parameters of the investigated bearings

Name		Unit	NU205	6205	6216
Bore diameter	d_i	mm	25	25	80
Outside diameter	D_a	mm	52	52	140
Bearing width	B	mm	15	15	26
Contact width	B_{AR}^*	mm	13	13	22
Diameter ratio (inner ring)	Q_{IR}	-	0.79	0.65	0.86
Diameter ratio (outer ring)	Q_{AR}	-	0.89	0.89	0.76
Quantity of rolling elements	Z	-	13	9	11
Dimensions of rolling elements	d_{WK} xb_{WK}	mm	Ø7.5 × 9	Ø7.9	Ø18.2
Static load rating	C_{0r}	kN	27.5	7.8	55
Dynamic load rating	C_r	kN	34.5	14.0	72.8
Fatigue limiting load	P_U	kN	3.3	0.5	2.2
Clearance group	*(C3)*	µm	35–60	13–28	30–58

TABLE 4 Radial load conditions of the experimental investigation for different bearings

Name		Unit	NU205	6205	6205—Dynamic	6216
Radial load	F_r	kN	8	8	6 ± 2 (10 Hz)	20
Related load	p_r	N/mm^2	10.3	10.3	7.7 ± 2.6	5.5
Load ratio	C/P	-	4.3	1.8	3.5 … 1.8	3.6

5 | ELASTIC INTERMEDIATE LAYER

The elastic layers in the bearing seats, which embed the bearing ring deformation that is typical of creep, have been studied for 2 sandwich materials. A thermoplastic layer with isotropic material behavior (see Figure 11 left) and a GRP layer with anisotropic material behavior (see Figure 11 right) were extensively studied using 3D kinematics simulation.

In essence, 3 influencing key variables could be detected based on the simulative tests with isotropic material behavior. These influencing variables (Young's modulus of the layer E_{FDD}, layer thickness, and coefficient of friction of the elastic layer) and their effect on creep are shown in Figure 12.

The effect of these layers in terms of the creep threshold is shown in Figures 13 and 14. The potential of this measure is clear. It was possible to obtain a 3-fold increase in the creep threshold compared with the untreated bearing. However, Figure 14 also shows that the GRP layer is significantly more effective for cylindrical roller bearings than for deep groove ball bearings.

The experimental studies of the elastic intermediate layers focused on GRP-coated bearings. For these measures, bearings 6205 and NU205 were investigated. The bearings were coated with a 0.4-mm-thick GRP layer that was built by several layers, applied with an angle of 90° against each other. In relation to the bearing axis, the fibers were arranged in an angle of 45°. Even though the bearings were grinded after the coating process the radial runout was slightly increased to 10 to 15 µm.

Table 5 shows the test results. The table includes information about the used bearing as well as the housing material, the outer ring clearance, the radial load, the outer ring revolutions, OR-Rev., with the shaft revolutions where the bearing stopped creeping (Lim. shaft rev.), and the total shaft revolutions for the test.

The results show that with a radial load of 6 kN, the deep groove ball bearings could not be prevented from bearing creep. The presence of lubricant in the contact area has no effect on bearing creep as the contact zone in the test with a sealed bearing (6205 2RSH) was cleaned before the test. For both experiments, the deep groove ball bearing creeped constantly during the whole test. Figure 15 shows the rotational speed of the outer ring and the cumulative outer ring revolutions for the test with the non-sealed bearing 6205 plotted against the shaft revolutions.

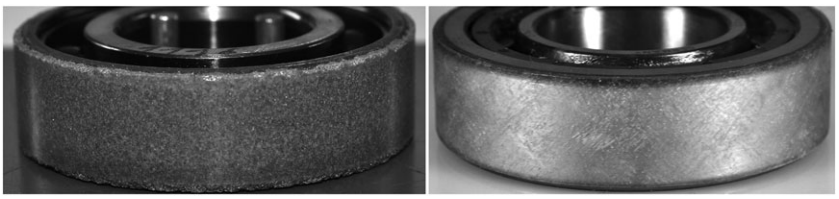

FIGURE 11 PEVAC layer (left) and GRP layer (right) on a deep-groove ball bearing of type 6205

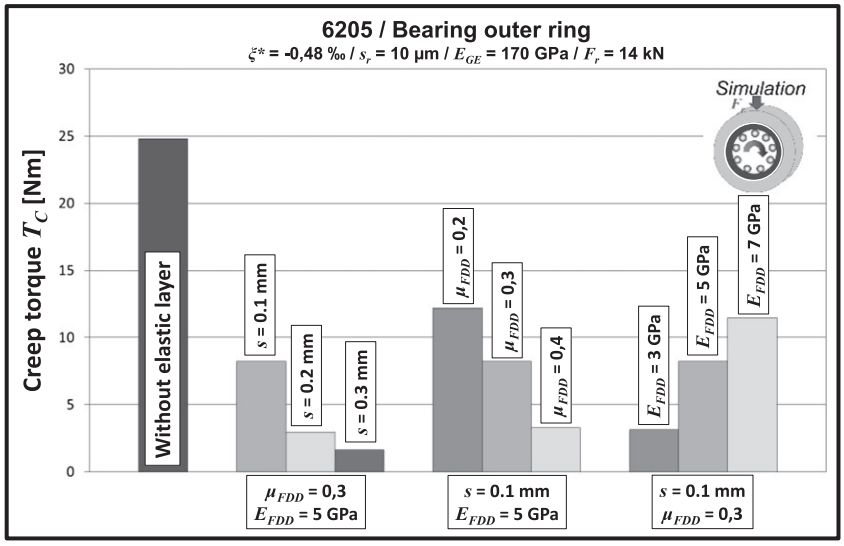

FIGURE 12 Comparison of creeping torque for different layer thicknesses s, varying coefficients of friction μ_{FDD} and varying Young's moduli E_{FDD} of the isotropic plastic layer

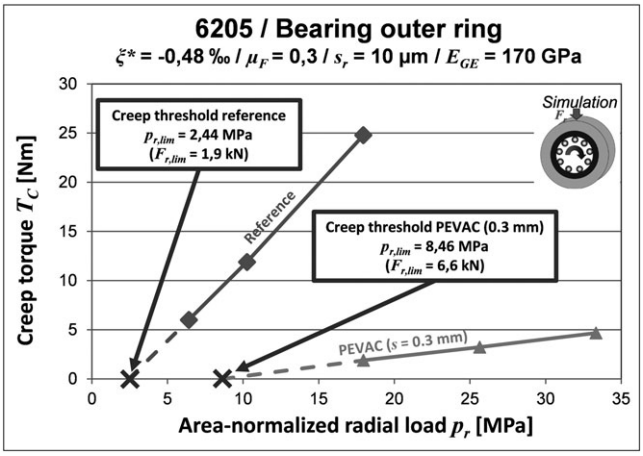

FIGURE 13 Comparison of creep thresholds for the reference and the PEVAC layer (bearing type 6205)

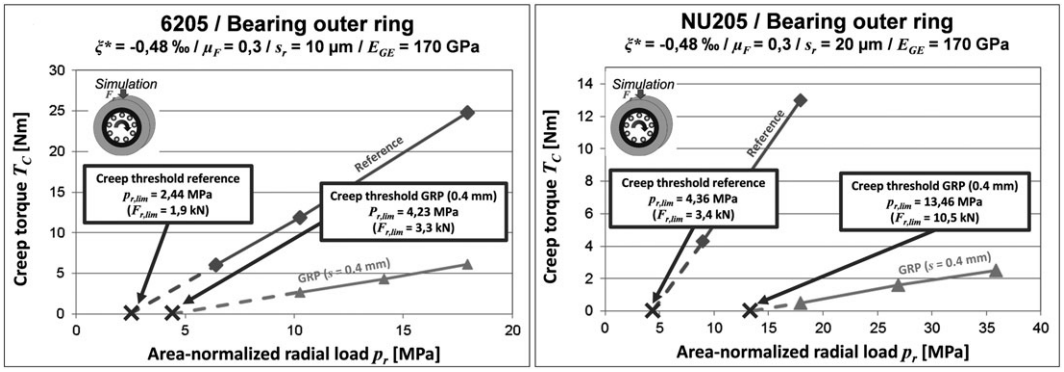

FIGURE 14 Comparison of creep thresholds for the reference and the GRP layer with a layer thickness of s = 0.4 mm (left: bearing 6205; right: bearing NU205)

TABLE 5 Experimental investigation of GRP layer with bearings 6205 and NU205

Bearing	Housing Material	Clearance U^*, µm	Radial Load, kN	OR Rev. u_{Ar}, −/Lim. Shaft Rev. u_{Grenz}, −	Shaft Rev. u_{Ges}, −
6205 C3	42CrMo4	−20 (ξ* = −0.38‰)	6	39.11 / >1 000 000	1 000 000
6205 C3 2RSH	42CrMo4	−22 (ξ* = −0.42‰)	6	34.32 / >1 000 000	1 000 000
NU 205	42CrMo4	−19 (ξ* = −0.37‰)	6	0	1 000 000
NU 205[a]	42CrMo4	−19 (ξ* = −0.37‰)	6	0.22 / 27 000	1 000 000

[a]Quantity of rolling elements reduced from 13 down to 7.

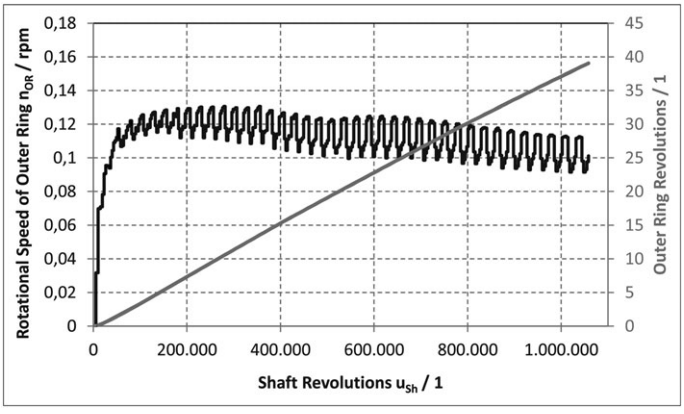

FIGURE 15 Bearing creep of a deep groove ball bearing 6205 with a GRP layer

It can be seen that the bearing starts to creep immediately after the start of the test with a short acceleration phase and then reaching off to a nearly constant rotational speed of approximately 0.1 rpm which led to 39 revolutions of the outer ring.

In the view of bearings NU205, the GRP layer was much more successful counteracting bearing creep. The first test shows no relative movement of the outer ring with a radial load of 6 kN. A second test was carried out with a reduced number of rolling elements, trying to decrease the bearing creep threshold. Even with only 7 instead of 13 rolling elements, the GRP layer prevented the bearing from continuous creeping. Only during the first 27 000 shaft revolutions, the outer ring twisted through 0.22 revolutions. Considering the components after the test (see Figure 16), it becomes clear that even if bearing creep is detected (left), the components were not significantly damaged by fretting corrosion or wear. Looking into the outside diameter of the bearings after the experiments, a reduction in the layer thickness of 10 μm with the sealed bearing was detected. Thus, it needs to be mentioned that this measure should not be used with the absence of lubricant in the contact area as there has been no decrease in the layer thickness with a lubricated contact area.

The experimental results correspond to the simulative investigation as the bearing creep threshold for GRP-coated deep groove ball bearing 6205 is 3.3 kN which is below the radial load that was applied during the tests. For the cylindrical roller bearings, the creep threshold is above the applied radial load at 10.5 kN.

With the PEVAC layer, only 1 test was made that could also confirm the simulative investigation as the bearing was prevented from creep at a radial load of 6 kN, see Table 6.

Looking at the components after the investigation, no significant damage is observed, see Figure 17.

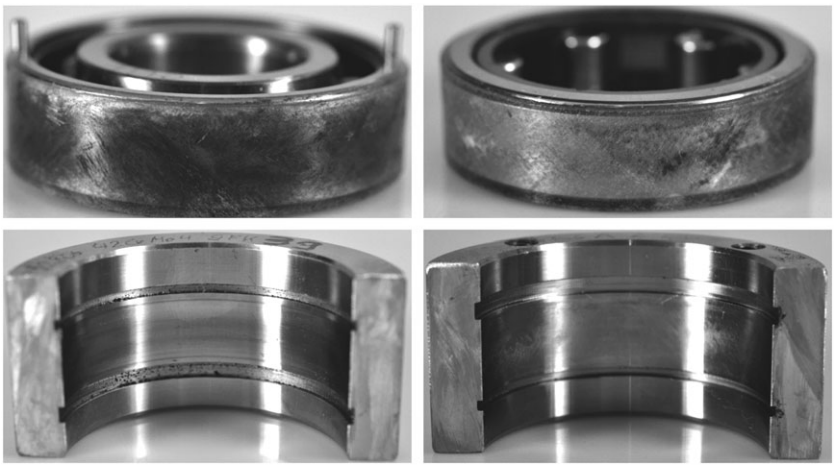

FIGURE 16 GRP-coated bearings and housings after test. Left: Creeped bearing 6205, right: Non-creeped bearing NU205 with reduced quantity of rolling elements

TABLE 6 Experimental investigation of PEVAC layer with deep groove ball bearing 6205

Bearing	Housing Material	Clearance U^*, μm	Radial Load, kN	OR Rev. u_{Ar}, −/Lim. Shaft Rev. u_{Grenz}, −	Shaft Rev. u_{Ges}, −
6205 C3	GJL-250	−1 (ξ^* = −0.02‰)	6	0	1 000 000

FIGURE 17 PEVAC-coated bearing and housing after test

6 | ADDITIONAL INTERMEDIATE STEEL RING

The intermediate steel ring (ISR) is fitted onto the outer ring of the bearing by an interference fit. This measure results in the superposition of 2 creep-inhibiting effects. The excess dimension (interference fit) in the contact joint between the bearing ring and the intermediate ring counteracts creep. Furthermore, creep motion in the contact joint between the housing and the intermediate ring is reduced by the absorbing and simultaneously stiffening effect of the intermediate ring. The bearing ring deformations typical of creep are embedded, and the remaining creep torque is transferred to the housing through a larger joint diameter. The studies with varying intermediate ring thicknesses (see Figure 18) illustrate the

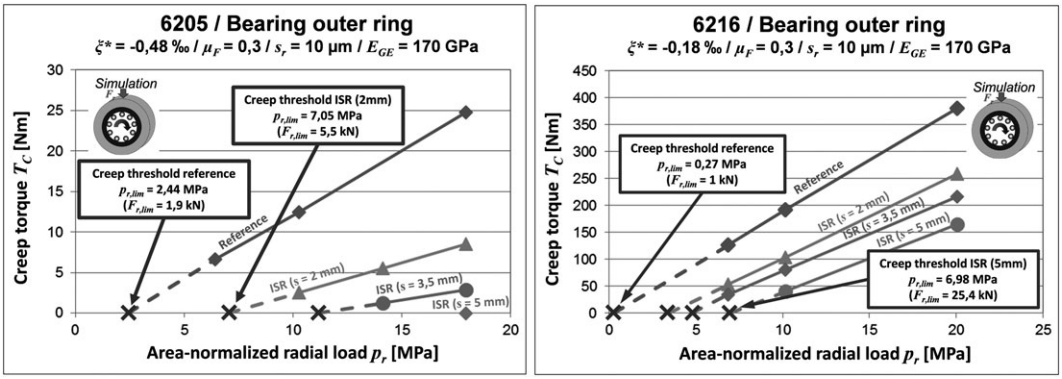

FIGURE 18 Creep torques arising with variations intermediate steel ring (ISR) thickness and the area-normalized radial load (left: bearing 6205; right: bearing 6216)

increase in the creep threshold and reduction in the creeping torque resulting from an intermediate ring in the bearing seat of deep groove ball bearings 6205 and 6216.

These studies were also performed for the cylindrical roller bearings of types NU205 and NU216. The area-normalized creep threshold is determined as a function of the ring-thickness ratio plotted in a diagram (see Figure 19). This diagram enables the practitioner to determine the necessary ring-thickness ratio as a function of the expected bearing load as well as the type and size of the bearing and therefore allows to calculate the required ring thickness using the following equation:

$$s = Q \cdot s_L$$

s – *required intermediate–ring thickness*
Q – *ring–thickness ratio*
s_L – *bearing–ring thickness*

The ring-thickness ratio was determined with conservative calculated creep thresholds, so that the designer is always on the safe side designing the bearing seat.

The interference fit between the bearing ring and the intermediate ring is dimensioned with the calculation model shown below. This model is based on the results of the project FVA 479 III "Lagersitze II."[2] This project illustrates the reduction in the creeping torque resulting from an interference fit.

The following equation enables the determination of the required pressure p_F.

$$p_F = \frac{p_r \cdot 0.3}{K_L \cdot \mu_F}$$

p_r – *Area – normalized radial load*
K_L – *Factor for type of bearing*
μ_F – *Coefficient of friction*

For the factor K_L, choose the following values depending on the type of the bearing:

Cylindrical roller bearing: $K_L = 6.8$
Deep groove ball bearing: $K_L = 12$

With this pressure, the required interference fit between the bearing ring and the ISR can be calculated with an analytical equation obtained from the shaft hub connection.[11]

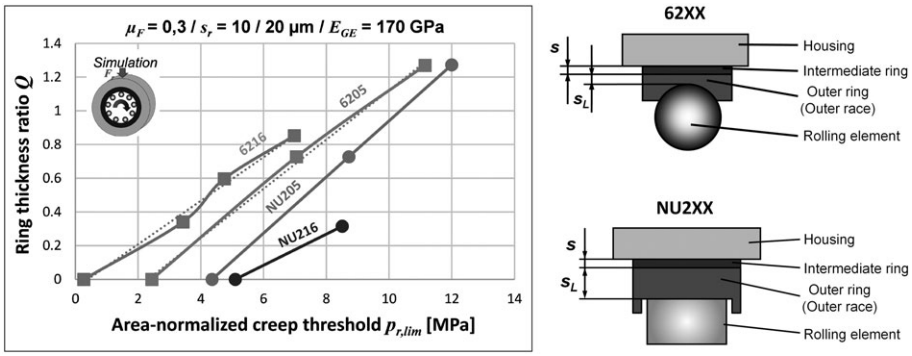

FIGURE 19 Ring-thickness ratio as a function of the related creep threshold for bearing types 6205, 6216, NU205, and NU216

For the experimental part of the investigation, the steel rings made up of 42CrMo4 are used with varying ring thicknesses of 2, 3.5, and 5 mm for bearing types 6205 and NU205, while the thickness of 2.5 and 5 mm for the bearings 6216 are used. As the creep threshold of a deep groove ball bearing is lower than the threshold of a cylindrical roller bearing, most of the tests were conducted with deep groove ball bearings. Table 7 gives an overview of the tests with ISRs and bearing types 6205 and NU205. The tests were conducted with different interferences between

TABLE 7 Experimental investigation of intermediate steel ring with bearings 6205 and NU205

Bearing	Housing Material	Ring Thickness, mm	Clearance ISR/Hous. U^*, µm	Interference ISR/OR U, µm	Radial Load, kN	OR rev. u_{Ar}, −/Lim. Shaft Rev. u_{Grenz}, −	Shaft Rev. u_{Ges}, −
6205	C45	5	−43 (ξ* = −0.83 ‰)	3 (ξ = 0.06 ‰)	8	0	1 000 000
6205	18CrNiMo7-6	5	−21 (ξ* = −0.40 ‰)	19 (ξ = 0.37 ‰)	8	0	1 000 000
6205	GJL-250	2	−22 (ξ* = −0.42 ‰)	39 (ξ = 0.75 ‰)	8	0	1 000 000
6205	GJL-250	3.5	−40 (ξ* = −0.68 ‰)	29 (ξ = 0.56 ‰)	8	0	1 000 000
NU205	GJL-250	2	−45 (ξ* = −0.80 ‰)	36 (ξ = 0.69 ‰)	8	0	1 000 000
6205	42CrMo4	3.5	−31 (ξ* = −0.53 ‰)	34 (ξ = 0.65 ‰)	8	0.11 / 34 000	1 000 000
6205	C45	5	−45 (ξ* = −0.73 ‰)	0 (ξ = 0.0 ‰)	8	0.11 / 45 000	500 000
6205	42CrMo4	2	−19 (ξ* = −0.34‰)	2 (ξ* = 0.04‰)	6	0	1 500 000
6205	GJL-250	2	−32 (ξ* = −0.57‰)	31 (ξ* = 0.60‰)	6 ± 2[a]	0	1 000 000
6205	GJL-250	3.5	−23 (ξ* = −0.39‰)	28 (ξ* = 0.54‰)	6 ± 2[a]	0.11 / 40 000	1 000 000

[a]Frequency: 10 Hz.

TABLE 8 Experimental investigation of intermediate steel ring with bearings 6216

Bearing	Housing Material	Ring Thickness, mm	Clearance ISR/Hous. U^*, µm	Interference ISR/OR U, µm	Radial Load, kN	OR rev. u_{Ar}, −/ Lim. Shaft rev. u_{Grenz}, −	Shaft Rev. u_{Ges}, −
6216	GJL-250	5	−31 (ξ* = −0.22‰)	4 (ξ* = 0.03‰)	20	0.2 / 40 000	1 000 000
6216	GJL-250	5	−30 (ξ* = −0.21‰)	1 (ξ* = 0.01‰)	20	0.26 / 90 000	1 000 000
6216	42CrMo4	2.5	−23 (ξ* = −0.16‰)	0 (ξ* = 0.0‰)	20	7.0 / >1 000 000	1 000 000
6216	42CrMo4	2.5	−20 (ξ* = −0.14‰)	10 (ξ* = 0.07‰)	20	2.4 / 200 000	1 000 000

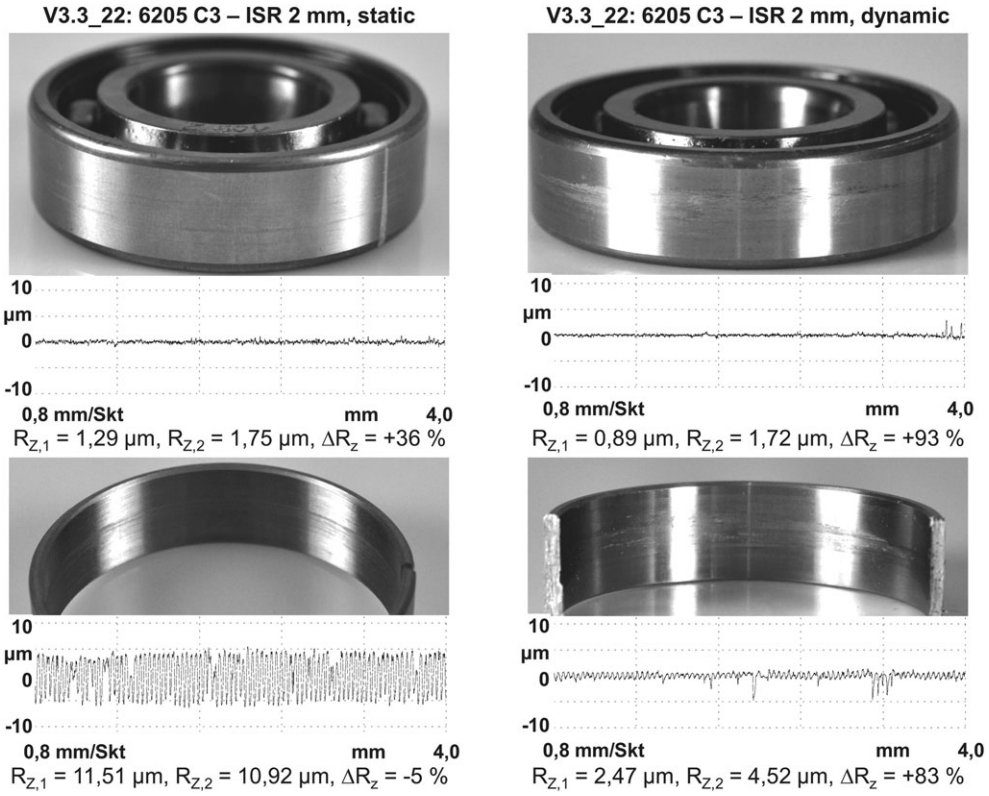

FIGURE 20 Bearing 6205 and 2 mm ISR after test with roughness measurement. Left: Test with static load. Right: Test with dynamic load

the bearing outer ring and the ISR. At the same time, different clearances between the ISR and the housing were chosen. The absolute values were measured and are shown within Tables 7 and 8. It can be seen that bearing creep was terminated for all tests with all ring thicknesses. In a few tests, there has been a minimal creep of approximately a tenth of a revolution. Here, it needs to be mentioned that the creep for these tests occurred during the first 45 000 shaft revolutions. After this, no further bearing creep was detected. Either with very small or even no nominal interference the bearings were prevented from creep. The last 2 rows show the tests with a dynamic radial load with an average value of 6 kN and amplitude of 2 kN that was applied with a frequency of 10 Hz. Even under these conditions, the ISR stopped the bearing creep.

Due to the nonexistent bearing creep, the bearings and the ISRs show almost no wear, see Figure 20. In these images, the bearing outer rings and ISRs of a test with a 2-mm ISR with static load (left) and dynamic load (right) are shown. It can be seen that for the static load conditions, no wear appeared at the components which is confirmed by the roughness measurement as shown below. After assessing the components of the test with the dynamic load, they show little wear on the surfaces. This is not a result of bearing creep but which is a consequence of micro-slippage that occurs in the contact area. The roughness measurement confirms this result as the average roughness R_z value increases for both parts. Comparing this with creeped bearings, a significant improvement is achieved.

After investigating the influence of the bearing size, deep groove ball bearings of type 6216 were used with ISR of 2.5 and 5-mm thickness. Table 8 shows the test results.

All tests were performed with a small interference of 10 µm or less between the ISR and the outer ring. Even with this small interference and the ISR of 5-mm thickness, the bearing creep has stopped after a little movement of maximum of a quarter revolutions after less than 90 000 shaft

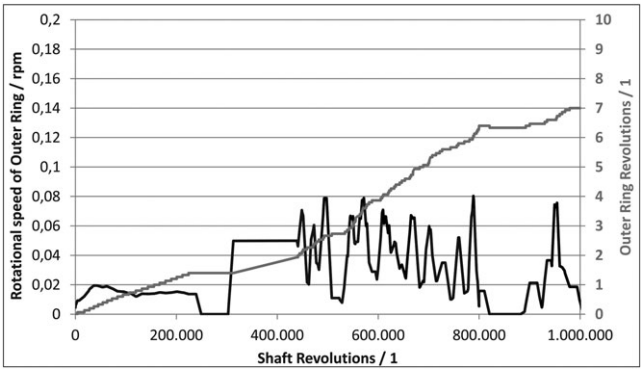

FIGURE 21 Bearing creep of a deep groove ball bearing 6216 with ISR 2.5 mm, interference 0 µm

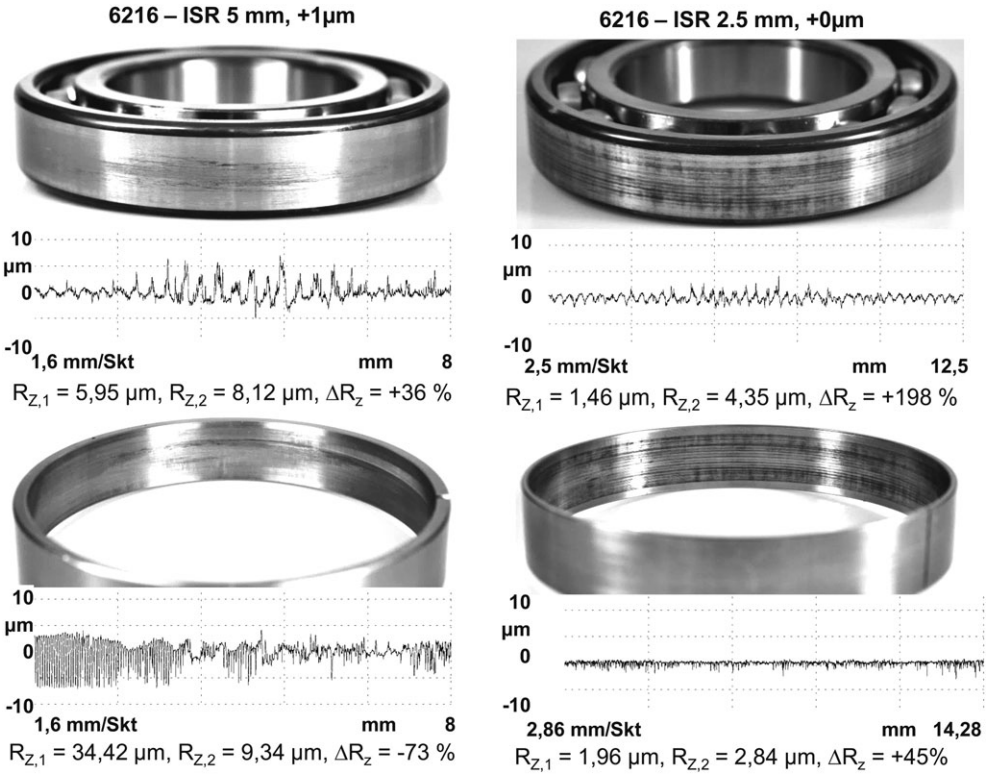

FIGURE 22 Bearing 6216 and ISR after test with roughness measurement. Left: Test with 5 mm ISR. Right: Test with 2.5 mm ISR

revolutions. For these bearings, an influence of the ISR thickness can be seen as the smaller ISR with 2.5 mm could not completely prevent the bearing from creeping. A test with an interference of 10 μm has stopped the bearing from creeping after 200 000 shaft revolutions and 2.4 OR revolutions. Here, the expected influence of the interference can be observed, as the ISR with a nominal interference 0 μm did not stop the bearing creep. During the 1 000 000 shaft revolutions, the OR performed 7.1 revolutions, see also Figure 21.

It can be seen that the bearing stopped creeping 2 times during the test for approximately 50 000 shaft revolutions but after creep has occurred again. So, no final stop of the bearing creep has taken place.

Comparing the demounted components of a test with a 5-mm ISR and a 2.5-mm ISR, the consequences of creep can be detected. The components with a 5-mm ISR show only a minimum of wear which is an effect of micro-slippage that occurs even without creep in the contact area. The surface roughness measurement verifies this result, as there is no significant increase in the average roughness R_z. As expected, the parts with the creeped bearing show the typical wear like fretting corrosion and abrasive wear as a consequence of the relative movement. This leads to an increased average surface roughness of the OR as well as the ISR, see Figure 22.

Considering these tests, it becomes clear that an ISR is a strong measure against rolling bearing creep. All tests with bearings 6205 and NU205 were successful. With all tested ring thicknesses and load conditions, the ISR could prevent the bearing from creeping. As the results show, even a small interference is sufficient to terminate creep which makes this measure easily applicable. Related to the tests with larger bearings 6216, it is confirmed that ISR are also an applicable solution for larger bearings. But, these tests have also shown that the ring thickness in relation to the bearing outer ring diameter needs to be considered. Therefore, the calculation methods were developed that are mentioned at the beginning of this chapter.

7 | CONCLUSION AND OUTLOOK

This article has presented examples of tribological, design, and positive-fit measures and their efficacies with respect to rolling bearing creep. Creep processes at bearing seats have been simulated using various FE analysis and laboratory tests subject to realistic boundary conditions, and these have been used to derive calculation models and design rules.

The calculation models and design rules presented here have been implemented in the bearing seat calculation software "SimWag2.1^{Z88}" as part of ongoing research work.[12] This provides designers with a tool whereby in future they will be able to detect and semi-automatically resolve rolling bearing creep early in the development phase.

Continuing research efforts with regard to bearing creep are concentrating on rolling-bearing-supported helical planetary gears.[13] In this case, in addition to creep in the circumferential direction, there can also be axial creep phenomena, which can cause severe damage in planetary gears. Ongoing research work is investigating the fundamental creep mechanisms of single-bearing and multiple-bearing systems and deriving calculation models for them. This model will make it possible to analyze planetary gears in terms of bearing creep and eliminate the latter as a possible source of failures in planetary gears.

ACKNOWLEDGEMENTS

The authors would like to thank the accompanying research association FVA for supporting IGF projects 15652 BG and 16985 BG. These research projects of the research association Forschungskuratorium Maschinenbau e.V. (FKM), Lyoner Strasse 18, 60528 Frankfurt am Main were funded via the AiF [German Federation of Industrial Research Associations] as part of the Program for the Promotion of Industrial Collective Research and Development (IGF) of the Federal Ministry for Economic Affairs and Energy based on a resolution of the German Bundestag.

ORCID

T. Schiemann http://orcid.org/0000-0002-8286-3277

REFERENCES

1. Leidich E, Sauer B, Maiwald A, Babbick T. Beanspruchungsgerechte Auslegung von Wälzlagersitzen unter Berücksichtigung von Schlupf- und Wandereffekten. Final report Forschungsvereinigung Antriebstechnik e.V., Frankfurt/M., Book 956, 2010
2. Leidich E, Sauer B, Maiwald A, Liebrecht J. Ringwandern bei angestellten Lagern und Radiallagern unter kombinierten Belastungen. Final report Forschungsvereinigung Antriebstechnik e.V., Frankfurt/M., Book 1097, 2014
3. Zhan J, Yukawa K, Takemura H. Analysis of bearing outer ring creep with FEM. In: *Advanced Tribology*. Berlin: Springer; 2010:237-238. ISBN:978-3-642-03652-1.
4. Podsceklodin M, Golubovskij W. Title Russian: investigation of slippage on rolling bearing outer rings under stationary load. *Kiev: Avtomobil'nyi transport*. 1973;10:64-67.
5. Stahl K, Otto M, Leonhardt C. Erweiterung von LAGER2 zur Dimensionierung von Wälzlagern in Industriegetrieben: Mechanische Kontaktgrößen und Tragfähigkeitskennwerte. Final report Forschungsvereinigung Antriebstechnik e.V., Frankfurt/M., Book 1185, 2016
6. Schiemann T, Leidich E. *Wälzlagerwandern in schrägverzahnten Planetenrädern–Einflussgrößen und Gegenmaßnahmen. VDI-Berichte 2308*. Düsseldorf: VDI Verlag; 2017:259-271. ISBN:978-3-18-092308-6.

7. Sauer B, Leidich E, Pörsch S, Schiemann T. Definition und Auslegung von konstruktiven und tribologischen Abhilfemaßnahmen gegen tangentiale Wanderbewegungen von Wälzlagerringen. Final report Forschungsvereinigung Antriebstechnik e.V., Frankfurt/M., Book 1153, 2015
8. Maiwald A. Numerische Analyse des Wanderverhaltens von Wälzlagerringen. Dissertation, Chemnitz University of Technology, 2013
9. *DIN ISO 281, Wälzlager—Dynamische Tragzahlen und nominelle Lebensdauer*. Berlin: Beuth Verlag; 2009.
10. Leidich E, Maiwald A. Research studies on irreversible relative movements (creeping) in rolling bearing seats regarding the influential parameters and the remedies. In: *Transactions on Engineering Technologies*. Springer: Dordrecht; 2014:549-562. ISBN:978-94-017-9114-4.
11. *DIN 7190, Pressverbände—Berechnungsgrundlagen und Gestaltungsregeln*. Berlin: Beuth Verlag; 2001.
12. Rieg F, Nützel F, Viebahn F. Auslegung von Abhilfemaßnahmen mit SimWag2.1^{Z88}. Forschungsvereinigung Antriebstechnik e.V., Frankfurt/M., Book 1249, 2017
13. Leidich E, Sauer B, Schiemann T, Pörsch S. Untersuchung des Wanderverhaltens von Wälzlagern in schrägverzahnten Planetenrädern. Frankfurt/M.: Forschungsvereinigung Antriebstechnik e.V., Research Project FVA 479 VI, IGF No.: 18311 BG, 2014 in progress

How to cite this article: Schiemann T, Pörsch S, Leidich E, Sauer B. Intermediate layer as measure against rolling bearing creep. *Wind Energy*. 2018;1–15. https://doi.org/10.1002/we.2170